Silicon (2022) 14:4249–4263
https://doi.org/10.1007/s12633-021-01167-4

ORIGINAL PAPER

Multi Response Optimization of ECDM Process Parameters for Machining of Microchannel in Silica Glass Using Taguchi–GRA Technique

Sadashiv Bellubbi[1,2] · Sathisha N[3] · Bijan Mallick[4]

Received: 2 February 2021 / Accepted: 13 May 2021 / Published online: 22 June 2021

Abstract
In this work, machining of microchannel in silica glass was successfully carried out using electro chemical discharge machining (ECDM) process. The experiments were planned according to L_{27} orthogonal array with applied voltage, stand-off distance (SOD), electrolyte concentration, pulse frequency and pulse-on-time (T_{ON}) as control factors. The material removal rate (MRR), overcut (OC) and tool wear rate (TWR) were considered as response characteristics. In this study the effects of control parameters on MRR, OC and TWR have been investigated. The increase in applied voltage, electrolyte concentration and pulse on time lead to the improvement in the output characteristics which is attributed to formation of heavily crowded hydrogen bubbles and further coalescence of hydrogen bubbles promotes the occurrence of sparks which resulted in higher values of MRR, OC and TWR. The multi-objective optimization of ECDM was carried out through grey relational analysis (GRA) method. Optimal combination of process parameters achieved from GRA was 45 V applied voltage, 25 wt.% electrolyte concentration, 1.5 mm SOD, 400 Hz pulse frequency and 45 μs T_{ON}. ANOVA for GRG study revealed that the applied voltage (70.33%) was most significant factor affecting output responses followed by electrolyte concentration (11.69%), pulse frequency (4.98%) and SOD (4.13%). Furthermore, the regression equations were formulated for the optimum combination to predict the collaboration and higher-order effects of the control parameters. In addition, confirmation test was conducted for the optimal setting of process parameters and the comparison of experimental results exhibited a good agreement with predicted values. The microstructural observation of machined surface for the optimum combination was carried out.

Keywords Electro chemical discharge machining (ECDM) · Silica glass · SOD · Electrolyte concentration · Grey relational analysis (GRA) · MRR · Overcut · Microchannel

1 Introduction

Nowadays, silica glass plays a significant role in potential areas like medical, MEMS, windows, optical lenses, crucibles, metrological instruments etc., attributed to its relatively higher thermal shock resistance and low coefficient of thermal expansion [1]. These applications call for the machining of microchannels which serve for the path for fluidic flow in microreactors, micropumps, bio medical devices and hydrogen fuel cells [2–4]. Howbeit, machining of microchannels in glasses through conventional techniques is difficult task owing to properties of glasses like high hardness and brittleness [5] and therefore non-traditional machining methods are called for machining these glasses. Several works in this regard have been reported for machining these glasses through USM, LBM, AJM, EDM, ECM, CHM, ECDM and WJM etc. Presently electro chemical discharge machining (ECDM) process is emerging as a cost effective substitute for ultrasonic machining, laser ablation and wet chemical etching to produce micro-features in non-conductive materials such as pyrex glass, borosilicate glass, silica glass, silicon wafers, quartz

✉ Sadashiv Bellubbi
bellubbisadashiv@gmail.com

[1] Department of Mechanical Engineering, Alva's Institute of Engineering and Technology, Moodbidri, Mangaluru, Karnataka 574225, India

[2] Department of Mechanical Engineering, Visvesvaraya Technological University, Belagavi, Karnataka, India

[3] Department of Mechanical Engineering, Yenepoya Institute of Technology, Moodbidri, Mangaluru, Karnataka 574225, India

[4] Department of Mechanical Engineering, Global Institute of Management and Technology, Krishnanagar, West Bengal, India

and ceramics [6]. ECDM process is a hybrid process which combines the features of ECM and EDM to produce micro-features like deep holes, narrow channels and small slots in non-conductive materials [2, 5]. Chemical and thermal phenomena are the primary mechanisms of this process to erode the material from the work material [7] thereby achieving the advantages of both; electrochemical dissolution as well as electric-discharge erosion from the work material [8].

In the past, several studies have been conducted to investigate the effects of the ECDM process parameters such as pulse frequency, applied voltage, current density, electrolyte concentration, anode to cathode distance, tool feed rate, pulse-on-time, duty cycle, stand-off-distance, different electrolytes, various tool materials etc. Dhanvijay et al. [9] performed ECD machining of fiberglass reinforced plastic with an equal proportion of NaOH and KOH mixture considered as electrolyte. Input process parameters such as voltage, duty factor, electrolyte concentration and tool rotation were optimized so as to obtain better MRR. The authors focused on experimentation and GRA technique of ECDM process with and without flow of electrolyte and concluded that with continuous flow of electrolyte, MRR increased marginally. Bellubbi et al. [10] machined microchannel in silica glass using ECDM process and it was noticed that error between predicted and experimental values of MRR, machining depth and overcut were 4.22%, 1.92% and 3.46% respectively. Priyaranjan et al. [6] focussed on machining of deep micro-holes in alumina by ECDM process. Authors reported the effects of voltage and tool feed rate on geometrical characteristics like depth, overcut, side wall profile of micro-hole along with tool wear. Experimental results confirmed that machining of alumina is difficult than the glasses which require higher voltage for machining.

Mallick et al. [11] analysed the MRR, WOC, SR and HAZ during micro-channelling in silica glass using ECDM process by considering various parameters and it was demonstrated that MRR, WOC and HAZ area enhanced with increase in applied voltage. Torabi et al. [12] created microchannel in polydimethylsiloxane (PDMS) using ECDM process and studied the effect of tool characteristics, electrolyte properties on the surface quality, surface roughness and dimensional accuracy of microchannel produced in PDMS. The machining of borosilicate glass [13, 14], alumina substrate [6], silica glass [1,10,15], pyrex glass and soda lime glass [16–18], fused silica and quartz [6], carbon fiber reinforced polymer (CFRP) [19] on hole geometry, overcut, HAZ, MRR, machining depth, circularity error, surface roughness, tool wear rate etc. have been investigated.

Optimization of control parameters plays a significant role and assists to identify the range of most effective parameter that controls the machining performance in ECDM. Several optimization methods were suggested to establish mathematical formulation between control parameters and response variables in ECDM process to produce micro-channels, micro-holes, texturing and grooves. Taguchi-GRA is one of the attractive optimization techniques employed by many investigators to establish a control over the uncertainty and optimize several responses in a process [20–22]. Taguchi-GRA is extensively employed for evaluating the degree of relationship between arrangements by grey relational grade (GRG). Several researchers have recently used GRA technique to optimize the combination of different process parameters on soda lime glass [23], quartz glass [24], fiber glass reinforced [9], borosilicate glass [25, 26], CFRP composites [19], silica (quartz) material [24], silicon wafer [27]. Works reported hitherto prove the effectiveness of Taguchi-GRA for optimizing ECDM process parameters; nevertheless, the available literature reveals the paucity of published works reported on micromachining of silica glass and relevant multi response optimization through GRA. In this work, the influence of control factors; applied voltage, pulse frequency, pulse-on-time, stand-off-distance and electrolyte concentration on response variables; MRR, OC and TWR have been investigated. Furthermore, multi response optimization of ECDM of silica glass through Taguchi-GRA has been proposed and the significance of process parameters was determined through ANOVA. Subsequently, the confirmation test was carried out by considering the optimal combination of process parameters.

2 Experimental Work

Recent developments in ECDM process comprises with micro-machining of ceramics, glass, composites, silicon wafer and quartz with enhanced output responses [13]. The performance of ECDM process in terms of width of cut, surface roughness, machining depth, TWR, MRR, heat affected zone, recast layer is mainly dependent on various factors like SOD, voltage, current density, electrolyte concentration, auxiliary electrode material, tool materials, electrolyte and pulse factors of supply.

2.1 Materials and Methods

In this research, silica glass of size $75 \times 26 \times 1.2$ mm^3 was used as the work material for experimentation. Table 1 presents the physical properties of silica glass used in the present work. The main composition of silica glass is SiO_2 that increases the resistance to thermal shocks [28]. The required ECDM facility for the experimentation was developed as shown in Fig. 1a which consists of power regulated supply, tool holder equipped with 3-axis movement, fixture for holding workpiece, electrodes and electrolyte container. The tool head movement was controlled by GRBL software. A Tungsten carbide tool of 250 μm diameter was considered

Table 1 Properties of silica glass [15]

Properties	Value
Tensile strength (N/m^2)	50×10^6
Thermal conductivity (W/m-K)	1.2
Elastic modulus (N/m^2)	72×10^9
Density (kg/m^3)	2.519×10^3
Thermal expansion (K^{-1})	0.54×10^{-6}
Melting temperature (°C)	1400
Refractive index	1.518

as cathode, graphite plate of 300 × 200 mm was used as auxiliary electrode (anode) and NaOH solution with varying concentrations was employed as electrolyte solution. NaOH electrolyte having most interesting properties compared to other electrolytes like NaCl, KOH, $NaNO_3$, NaF, H_2SO_4 and HCl [5]. Figure 1b shows typical photograph of the silica glass with micro machined groove.

The machining parameters during pilot experiments were selected based on literature review and initial experiments were conducted by one time approach. After performing the pilot experiments, it was noticed that the viable range of applied voltage was 45-55 V, the electrolyte concentration range 10-25 wt.%, the SOD 0.5–1.5 mm, the pulse frequency 200-400 Hz and the pulse on time 45-55 μs. The parameter design in present work is based on three levels for each machining parameter as shown in Table 2. The stand-off-distance was set using slip gauges between the work material and tool tip. Inter-electrode-gap and machining time were kept constant as 40 mm and 20 min respectively for all trials.

The most prominent output responses were identified and selected as MRR, OC and tool wear rate (TWR). MRR and TWR were determined in terms of material eroded per unit time. The samples and tools in each trial were precisely weighed before and after machining using a digital electronic balance (Make: Mettler Toledo, India) with 0.01 mg resolution. The overcut was measured using Leica microscope at various locations throughout the length of microchannel (Fig. 2) and the average values have been considered. Machined surfaces were also subjected to micrographic observations through scanning electron microscope; SEM (Model: JEO JSM–638OLA from JEOL, Japan). Figure 3 showing field emission scanning electron microscopy (FESEM) demonstrates the depth of machined surface of the experiment no. B5, machining depth observed in the range from 140 to 400 μm.

2.2 Working Principle of ECDM Process

The ECDM setup comprises of a primary tool electrode as cathode and a secondary metallic sheet as auxiliary electrode (anode) separated by an inter-electrode gap filled with electrolyte solution and regulated DC power supplied between both the electrodes.

The cathode tool is relatively much smaller than the auxiliary electrode [29]. The work sample is placed below the tool and submerged in electrolyte solution as in Fig. 4a. As the voltage is applied across the electrodes, the electrochemical reactions occur in the electrolyte solution when the applied voltage crosses the critical value which is dependent on geometry and electrolyte concentration [5, 19]. Continued voltage supply and high current density boosts the electro chemical reactions and results in the formation of hydrogen bubbles in the vicinity of the tool [30] (Fig. 4b). The high density of hydrogen bubbles forms a casing around tool electrode (Fig. 4c). This casing behaves as dielectric between cathode tool and electrolyte solution, as the applied potential crosses the dielectric power of gas film, the spark is persuaded around tool electrode as shown in (Fig. 4d). Therefore, the work material beneath the tool electrode softens due to spark energy generated by these discharges probably contribute to erode the material by chemical etching and thermal erosion. As a result spark discharges promise a sequence of micro erosions in the layer of work piece, so that micro quantities of material takes place from work material continuously [14, 15].

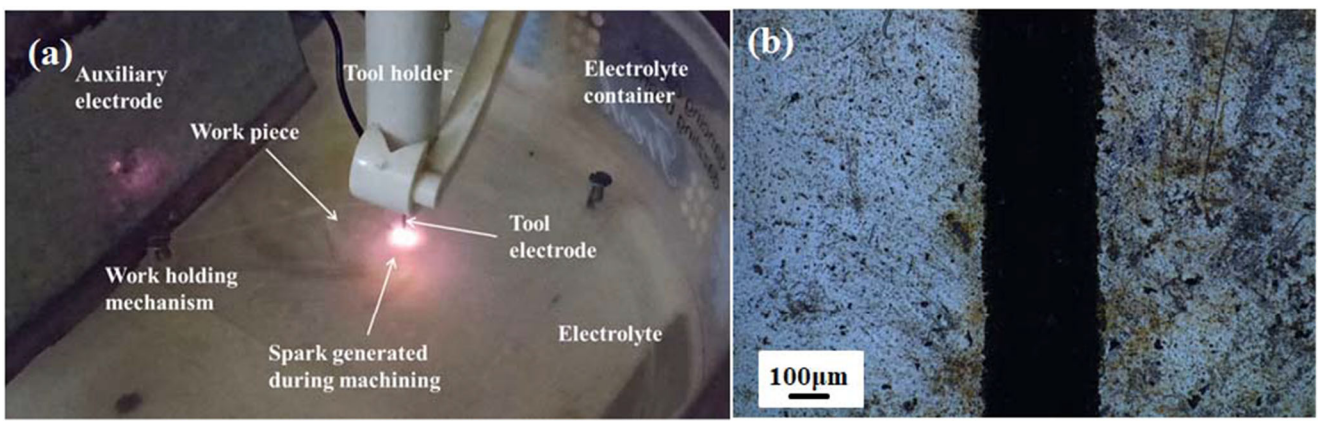

Fig. 1 Images of **a** ECDM **b** Optical image of Silica glass with micro-channel

Table 2 Machining parameters and their levels

Parameters	Unit	Factor	Level 1	Level 2	Level 3
Applied voltage	V	A	45	50	55
Electrolyte concentration	wt.%	B	10	17.5	25
Stand-off-distance	mm	C	0.5	1.0	1.5
Pulse frequency	Hz	D	200	300	400
Pulse-on-time	µs	E	45	50	55

2.3 Genichi Taguchi Method

The Taguchi OA lessens the fewer number of trials [31] and hence, time and cost essential for the experimentation. Commonly, based on the process parameters and their levels, more number of trials needs to be conducted as per traditional strategy. The intention behind selection of Taguchi-OA is to afford for the optimum level of each parameter so as to decide the relative contribution of individual parameter using ANOVA [20, 32]. The necessary number of experiments is chosen based on the degrees of freedom (DF) of individual factors and the addition DF of their interaction factors. The number of rows of an orthogonal array must be at least equivalent or greater than DF united with the selected factors i.e. the control variables and their interactions. In the present study 23 experiments have to be conducted as per total DF however, the nearest OA of design is L_{27}. Hence, L_{27} OA is selected for the experimentation. The experimental design in the present work was planned using Minitab-17 software as shown in Table 3.

2.4 Grey Relational Analysis (GRA)

The GRA has provided the information that, any experimental analysis provides complete precise information called white; else the analysis contains lack of information named as black. For instance the analysis is combination of both, then it is called grey and such analysis is termed as grey relational analysis [21, 33]. While optimizing through Taguchi's approach, single response function can be optimized, GRA is the most suitable technique to obtain the optimal process parameters on multi response characteristics [34]. So that the obtained result gives better MRR, low OC and low TWR. Instead of having various optimized results, GRA provides single optimum combination of parameters for better MRR, OC and TWR. This technique involves normalization of the obtained results to find grey relational coefficients (GRCs) and then grey relational grades (GRGs) [35]. The combination of parameters with highest GRG is closest to optimum solution and considered as best possible setting of parameters. Furthermore, the ANOVA is executed to predict the optimum GRG. GRA have been employed by various researchers in their related field for multi-objective optimization of process parameters [36]. Figure 5 illustrates the steps involved in GRA.

3 Results and Discussion

Experimentation carried out to study the influence of control factors on MRR, OC and TWR according to design matrix shown in Table 3. Further, ANOVA was performed to study the significance and individual contribution of each control factors towards MRR, OC and TWR as shown in Table 4. Consequently, GRA has been performed to achieve the best possible combination of process parameters resulting in optimal setting followed by confirmation test to ensure the same.

3.1 Influence of Process Parameters on Response Characteristics

In general, any increment in voltage enhances in magnification of the coalescence of gas bubbles that boosts the intensity of spark over the work material. As a result, higher material

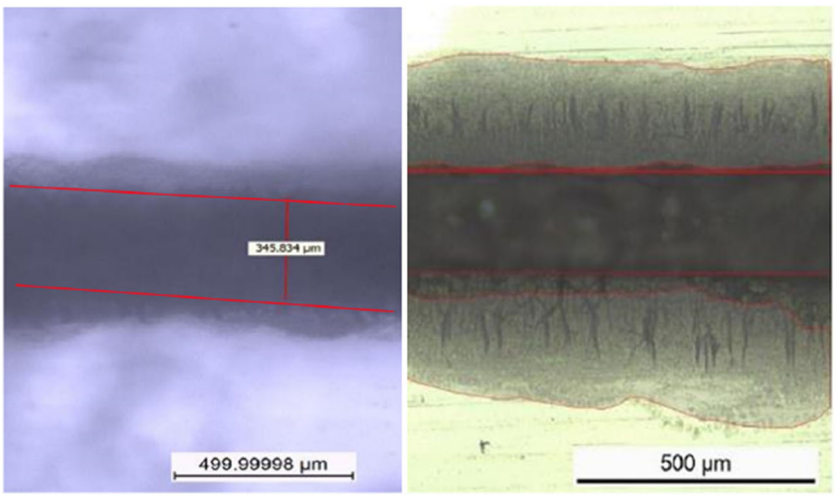

Fig. 2 OM images depicting the measurement of overcut in the machined microchannel

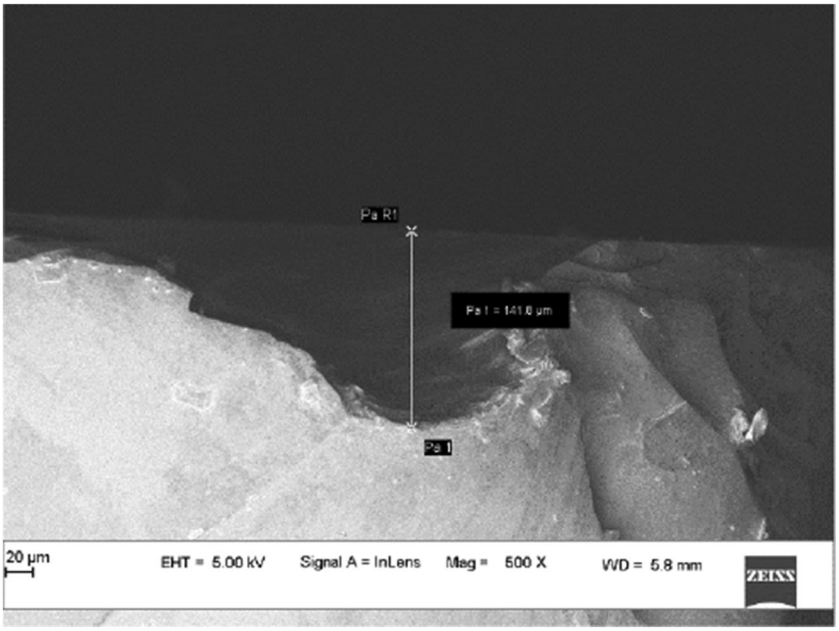

Fig. 3 FESEM image showing the measurement of depth of the machined microchannel

removal takes place due to larger thermal energy input. An increase in electrolyte produces the OH ions which escalates its electrical conductivity. Due to the high melting point of the Tungsten Carbide tool, the amount of molten material removed on the tool is very low compared to the workpiece [30]. As SOD increases, the spark generation between tool and workpiece reduces hence every discharge removes very little amount of material from tool electrode and work sample [37]. Influence of process parameters was analyzed based on the results obtained in Table 3. Also ANOVA was performed to find contribution of individual parameters on responses as shown in Table 4. Accordingly in the following sections the effect of process parameters and their individual contributions on MRR, OC and TWR has been elucidated.

3.1.1 Effect of Control Factors on MRR

It was noticed from Table 3 that, the MRR enhanced with increase in applied voltage. This is attributed to the formation of heavily crowded hydrogen bubbles along the edge of cathode tool. The coalescence of hydrogen bubbles promotes the occurrence of sparks which resulted in higher MRR. As the voltage

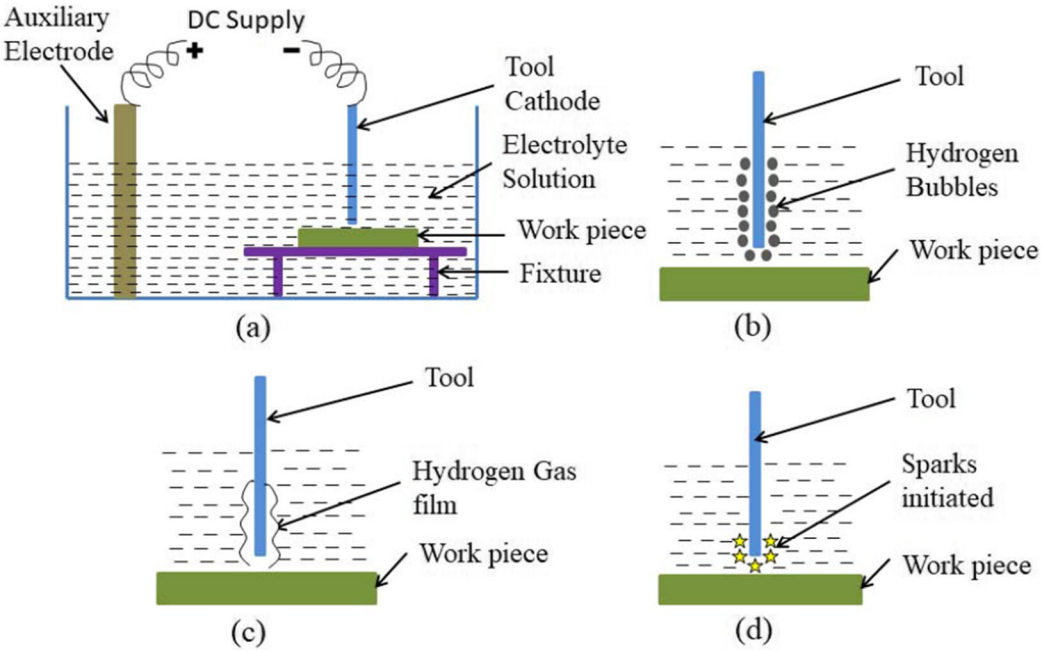

Fig. 4 **a** Schematic view of ECDM setup **b** Hydrogen bubbles formation **c** Hydrogen gas film formation **d** Spark initiation

Table 3 L_{27} orthogonal array layout with response variable

Run No.	Input parameters					Output responses		
	Applied Voltage (V)	Electrolyte Conc. (wt.%)	SOD (mm)	Pulse frequency (Hz)	Pulse-on time (μs)	MRR (mg/h)	OC (μm)	TWR (mg/h)
1	45	10	0.5	200	45	56.325	124.717	0.112
2	45	10	0.5	200	50	57.305	128.644	0.116
3	45	10	0.5	200	55	58.970	131.587	0.119
4	45	17.5	1	300	45	58.420	130.119	0.117
5	45	17.5	1	300	50	59.010	131.060	0.118
6	45	17.5	1	300	55	62.370	139.432	0.126
7	45	25	1.5	400	45	49.040	108.951	0.096
8	45	25	1.5	400	50	51.820	114.960	0.102
9	45	25	1.5	400	55	53.050	117.488	0.105
10	50	10	1	400	45	69.860	155.694	0.142
11	50	10	1	400	50	71.950	160.523	0.147
12	50	10	1	400	55	74.010	165.235	0.152
13	50	17.5	1.5	200	45	75.870	168.723	0.156
14	50	17.5	1.5	200	50	76.765	170.835	0.158
15	50	17.5	1.5	200	55	83.900	186.855	0.174
16	50	25	0.5	300	45	100.190	220.300	0.207
17	50	25	0.5	300	50	77.560	165.512	0.158
18	50	25	0.5	300	55	84.940	189.467	0.176
19	55	10	1.5	300	45	69.275	154.505	0.141
20	55	10	1.5	300	50	75.910	168.810	0.156
21	55	10	1.5	300	55	76.640	178.041	0.165
22	55	17.5	0.5	400	45	81.250	181.024	0.168
23	55	17.5	0.5	400	50	83.820	186.733	0.173
24	55	17.5	0.5	400	55	86.715	193.222	0.180
25	55	25	1	200	45	76.680	170.658	0.158
26	55	25	1	200	50	82.765	184.313	0.171
27	55	25	1	200	55	102.470	231.325	0.218

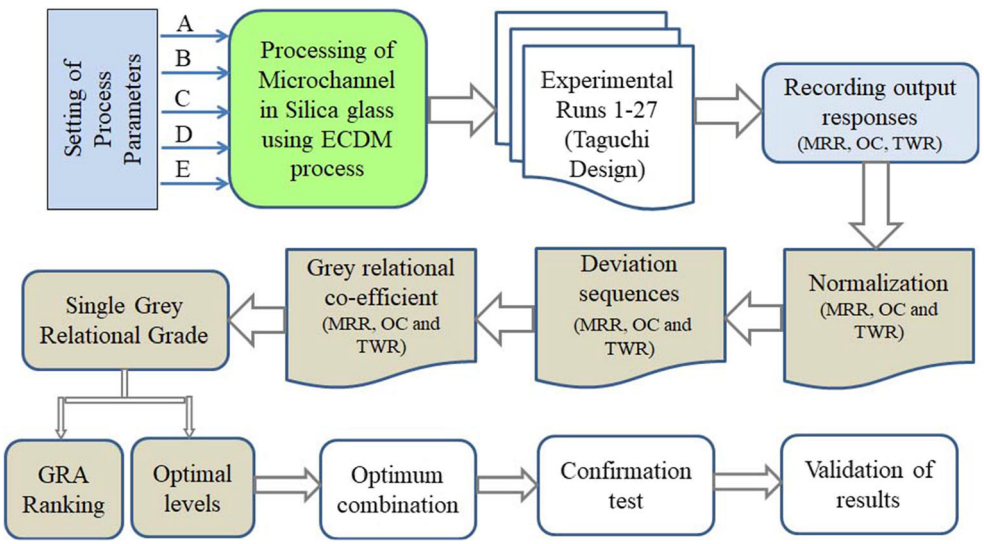

Fig. 5 Steps involved in GRA method

Table 4 Results of ANOVA for response characteristics

Response variable	Source	DF	Seq SS	Adj MS	% Contribution	Remarks
Material removal rate	Applied voltage (V)	2	3575.2	1787.58	70.13	Significant
	Electrolyte Conc. (wt.%)	2	300.7	150.34	5.90	Significant
	SOD (mm)	2	315.5	157.73	6.19	Significant
	Pulse frequency (Hz)	2	160.4	80.20	3.15	Insignificant
	Pulse on time (μs)	2	157.8	78.91	3.10	Insignificant
	Residual Error	16	588.4	36.77		
	Total	26	5097.9			
Overcut	Applied voltage (V)	2	17,945.8	8972.9	70.22	Significant
	Electrolyte Conc. (wt.%)	2	1221.0	610.5	4.78	Insignificant
	SOD (mm)	2	1324.0	662.0	5.18	Insignificant
	Pulse frequency (Hz)	2	818.5	409.3	3.20	Insignificant
	Pulse on time (μs)	2	1060.4	530.2	4.15	Insignificant
	Residual Error	16	3186.8	199.2		
	Total	26	25,556.4			
Tool wear rate	Applied voltage (V)	2	0.0179	0.0089	70.44	Significant
	Electrolyte Conc. (wt.%)	2	0.0013	0.0006	5.10	Insignificant
	SOD (mm)	2	0.0014	0.0007	5.44	Significant
	Pulse frequency (Hz)	2	0.0009	0.0004	3.39	Insignificant
	Pulse on time (μs)	2	0.0010	0.0005	3.97	Insignificant
	Residual Error	16	0.0029	0.0002		
	Total	26	0.0254			

increases beyond the 55 V, the viscosity of glass decreases progressively with an increase in temperature which leads to remove more material from workpiece [38]. Likewise, the increase in concentration boosted the MRR. The high electrolyte concentration stimulates the kinetics of electrochemical reactions. As a result, the electrochemical reaction accelerates and leads to the increase in coalescence rate of hydrogen bubbles thereby producing more discharge energy in machining area. This high discharge produces melting and vaporizes work material. On the contrary, MRR decreases as SOD increases; this is because as the gap between tool and workpiece increases the kinetics of electrochemical reactions diminishes, resulting in decrease of sparking phenomenon. Further it was noticed that, with increase in pulse frequency, the length of the on-time reduces resulting in lower MRR. Whereas, shorter on-times erodes very little material and generate smaller craters [37]. These observations made are consistent with those investigated by other researchers [13, 19]. From ANOVA study, it was noticed that applied voltage (70.13%) is the mostly influencing factor affecting MRR. The SOD (6.19%) and electrolyte concentration (5.90%) marginally influences the MRR as in Table 4.

3.1.2 Effect of Control Factors on Overcut

The overcut increases with rise in voltage supply and electrolyte concentration while, it decreases with increase in SOD and pulse frequency. As the applied voltage increases the thickness of hydrogen gas envelope increases around the cathode due to thicker hydrogen bubbles [30]. Therefore, sparking at the sides of cathode electrode upholds overcut as shown in Fig. 6 which depicts the typical cases observed with smaller and larger overcuts. The increase in electrolyte increases stray sparking over vicinity of tool electrode which leads to overcut. During the pulse interval, the regulated power supply is cut off and the hydrogen bubble formation is ceased thereby momentary extinction of sparks occurs which leads in smaller overcut. By choosing high frequency pulse parameters and lesser duty ratios, the surface roughness and overcut of machined area can be reduced [37]. From Table 4, it was observed from ANOVA that the applied voltage (70.22%) is the most significant factor influencing overcut, followed by the SOD (5.18%) and the electrolyte concentration (4.78%). In similar works, Garg et al. [19] reported that overcut rises with increase in voltage and concentration.

3.1.3 Effect of Control Factors on TWR

It was observed that the influence of control factors on TWR followed the trend which was similar to as that observed in case of MRR and OC. The TWR increased with respect to increase in applied voltage, electrolyte concentration and T_{ON}. However, TWR decreased with higher values of SOD and

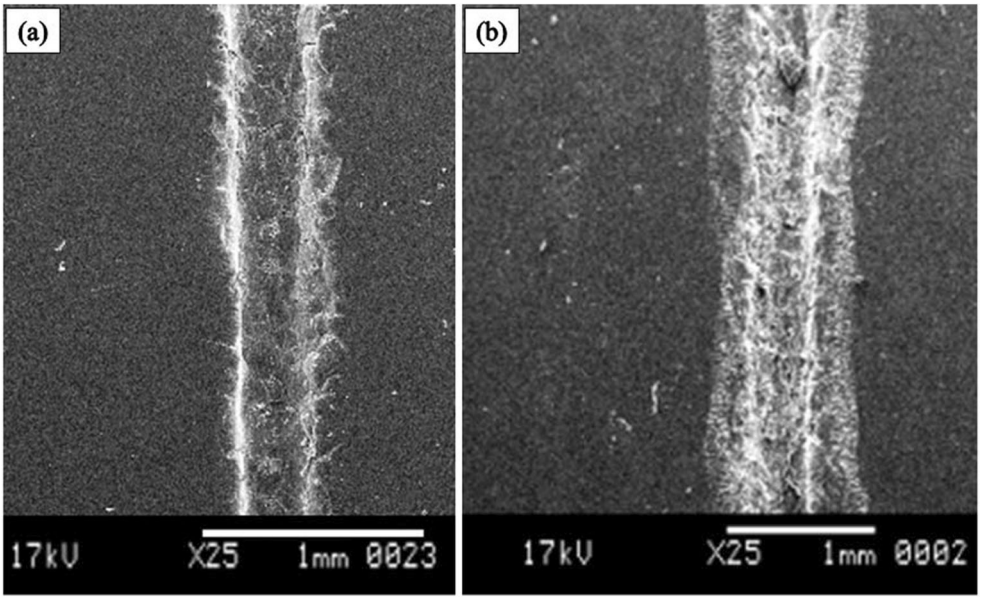

Fig. 6 Typical SEM micrographs of microchannel showing effect of process parameters on overcut **a** minimum overcut **b** maximum overcut

pulse frequency. As the voltage and concentration increase, heat generation in the machining zone is escalated which leads to higher MRR as well as TWR. Jui et al. [39] reported that TWR reduced with the dropping of the electrolyte concentration. The heat transmitted to the workpiece increases with the electrolyte concentration which (heat transmitted) further is also accountable for the loss of tool material. The decrease in TWR with respect to increase in SOD is due to the fact that each spark occurred between the neighboring point of the cathode tool and work sample and each sparks melts a smaller quantity of material from both [37]. Table 4 shows that factor applied voltage (70.44%) is the most influential factor followed by stand-off-distance (5.44%) and electrolyte concentration (5.10%) on overcut based on ANOVA by considering 95% confidence level. Figure 7 shows the SEM (Make: Zeiss) micrograph of ruptured WC tool tip. Since sparking occurs at the tip of tool, it is subjected to relatively higher temperature and thermal cycle compared to the stem portion of tool electrode and hence is more susceptible for failure. It was observed that micro size of tool material worn out due to increase in voltage and concentration. A part of discharge energy is transferred to the cathode surface which fuses and evaporates a small portion of the cathode material. Since, the tool tip is the sharpest edge, it receives large amount of thermal energy and therefore, subjected to higher wear compared to the stem portion of the tool [30].

3.2 Multi Response Optimization through Taguchi-GRA

The assessment of optimal process factors for a precise machining practice is an important assignment for researchers [19]. Most of the engineering systems involve multiple response characteristics to be determined however; a single combination of input factors may be optimal for single response but the same combination of input factors may not yield best results for the other responses. Thus, it is required

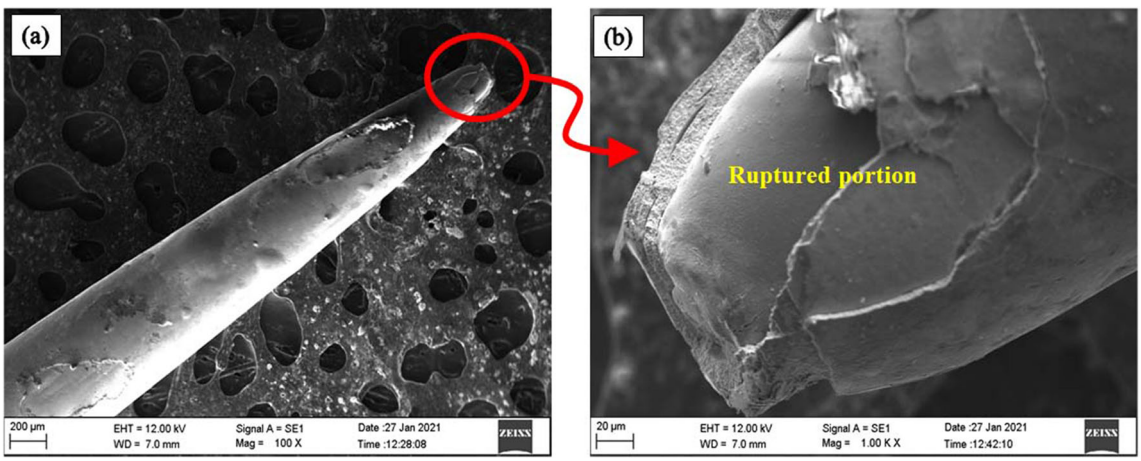

Fig. 7 Typical SEM micrograph showing tool wear **a** tool tip **b** magnified view

Table 5 Computing GRCs, GRGs and ranking

Run No.	Output responses			Normalized			Deviation sequence			Grey Relation Co-efficient			GRG	GRA Rank
	MRR (mg/h)	OC (μm)	TWR (mg/h)	MRR	OC	TWR	MRR	OC	TWR	MRR	OC	TWR		
1	56.325	124.717	0.112	0.136	0.871	0.872	0.864	0.129	0.128	0.367	0.795	0.796	0.653	4
2	57.305	128.644	0.116	0.155	0.839	0.839	0.845	0.161	0.161	0.372	0.757	0.757	0.628	5
3	58.970	131.587	0.119	0.186	0.815	0.810	0.814	0.185	0.190	0.380	0.730	0.724	0.612	8
4	58.420	130.119	0.117	0.176	0.827	0.825	0.824	0.173	0.175	0.378	0.743	0.740	0.620	6
5	59.010	131.060	0.118	0.187	0.819	0.817	0.813	0.181	0.183	0.381	0.735	0.732	0.616	7
6	62.370	139.432	0.126	0.249	0.751	0.757	0.751	0.249	0.243	0.400	0.667	0.673	0.580	9
7	**49.040**	**108.951**	**0.096**	**0.000**	**1.000**	**1.000**	**1.000**	**0.000**	**0.000**	**0.333**	**1.000**	**1.000**	**0.778**	**1**
8	51.820	114.960	0.102	0.052	0.951	0.948	0.948	0.049	0.052	0.345	0.911	0.905	0.720	2
9	53.050	117.488	0.105	0.075	0.930	0.927	0.925	0.070	0.073	0.351	0.878	0.873	0.700	3
10	69.860	155.694	0.142	0.390	0.618	0.620	0.610	0.382	0.380	0.450	0.567	0.568	0.529	13
11	71.950	160.523	0.147	0.429	0.579	0.582	0.571	0.421	0.418	0.467	0.543	0.545	0.518	14
12	74.010	165.235	0.152	0.467	0.540	0.543	0.533	0.460	0.457	0.484	0.521	0.523	0.509	16
13	75.870	168.723	0.156	0.502	0.512	0.511	0.498	0.488	0.489	0.501	0.506	0.505	0.504	18
14	76.765	170.835	0.158	0.519	0.494	0.493	0.481	0.506	0.507	0.510	0.497	0.497	0.501	20
15	83.900	186.855	0.174	0.652	0.363	0.364	0.348	0.637	0.636	0.590	0.440	0.440	0.490	24
16	100.19	220.300	0.207	0.957	0.090	0.093	0.043	0.910	0.907	0.921	0.355	0.355	0.544	11
17	77.560	165.512	0.158	0.534	0.538	0.489	0.466	0.462	0.511	0.517	0.520	0.494	0.510	15
18	84.940	189.467	0.176	0.672	0.342	0.343	0.328	0.658	0.657	0.604	0.432	0.432	0.489	26
19	69.275	154.505	0.141	0.379	0.628	0.630	0.621	0.372	0.370	0.446	0.573	0.575	0.531	12
20	75.910	168.810	0.156	0.503	0.511	0.511	0.497	0.489	0.489	0.501	0.505	0.505	0.504	17
21	76.640	178.041	0.165	0.517	0.435	0.431	0.483	0.565	0.569	0.508	0.470	0.468	0.482	27
22	81.250	181.024	0.168	0.603	0.411	0.411	0.397	0.589	0.589	0.557	0.459	0.459	0.492	21
23	83.820	186.733	0.173	0.651	0.364	0.365	0.349	0.636	0.635	0.589	0.440	0.440	0.490	25
24	86.715	193.222	0.180	0.705	0.311	0.312	0.295	0.689	0.688	0.629	0.421	0.421	0.490	23
25	76.680	170.658	0.158	0.517	0.496	0.495	0.483	0.504	0.505	0.509	0.498	0.498	0.501	19
26	82.765	184.313	0.171	0.631	0.384	0.384	0.369	0.616	0.616	0.576	0.448	0.448	0.491	22
27	102.47	231.325	0.218	1.000	0.000	0.000	0.000	1.000	1.000	1.000	0.333	0.333	0.556	10

to obtain an optimal combination of the control factors to yield a system with optimum quality characteristics. In section 3.1, GRA was implemented to resolve the problem of multiple quality characteristics [40] since MRR, OC and TWR were not interconnected mutually and independent with process parameters. Consequently, optimization method was extended for the complete estimation of multiple quality characteristics by producing microchannel in silica glass using ECDM process through GRA. The performance of ECDM process was enhanced by defining the objective as to maximize the MRR and minimize the overcut and TWR of machined section. This method determined that experimental trial with highest GRG is closest to optimum solution. The various steps followed in this method as discussed in following sections.

3.2.1 Normalizing the Data

For normalization of data for the MRR, the larger-the-better performance characteristic was considered and is expressed in Eq. 1. On the other hand for OC and TWR, the smaller-the-better performance characteristic was considered, and the same has been expressed in Eq. 2 [41].

$$X_i = \frac{Y_i - Y_{min}}{Y_{max} - Y_{min}} \tag{1}$$

$$X_i = \frac{Y_{max} - Y_i}{Y_{max} - Y_{min}} \tag{2}$$

where X_i is the normalized value, Y_i is the measured response value (i = 1, 2, 3….. 27 trials), Y_{min} and Y_{max} are minimum and maximum values of respective responses.

3.2.2 Calculation of Deviation Sequence

Deviation sequence is the difference between the reference value and normalized value obtained in the section 3.2.1, obtained value lies between 0 to 1. Deviation sequence was calculated using Eq. 3.

$$\Delta_i = [X_r - X_i] \tag{3}$$

where, Δ_i is the deviation sequence, X_r is the reference value considered as one [21] and X_i is the normalized value obtained.

3.2.3 Computation of Grey Relational Co-Efficient (GRC)

The GRCs of MRR, OC and TWR were computed by using the Eq. 4. ζ is distinguishing coefficient. Lesser the value of ζ, greater is the distinguishing capacity. In this study, value of ζ assumed in the range of $0 < \zeta < 1$ i.e. $\zeta = 0.5$.

$$GRC = \xi_i = \frac{\Delta_{min} - \zeta\Delta_{max}}{\Delta_i - \zeta\Delta_{max}} \tag{4}$$

where $\xi_i$is the GRC, Δ_i is the deviation sequence of i^{th} trial, Δ_{min} and Δ_{max} are smallest and largest values of Δ_i for respective responses.

3.2.4 Computation of Grey Relational Grade (GRG)

GRG was computed by averaging the GRC values related to each performance characteristic. GRG values were computed using Eq. 5 [20].

$$GRG = \gamma_i = \frac{1}{n}\sum_1^n \xi_i \tag{5}$$

Where ξ_i is the GRC, n is number of response variables i.e. 3 (MRR, OC and TWR). The larger GRG provides better performance characteristics [20, 21], which provides optimum MRR, OC and TWR. Further, GRG values are ranked from higher to lower. The results obtained from various steps of Taguchi-GRA are tabulated in Table 5.

From the grey analysis, it has been observed that seventh trial has maximum value of GRG and it is also shown in Fig. 8. Hence the experimental trial 7 was ranked as first. Therefore, in this work, out of 27 experiments trial 7 was considered as the best run. The process parameters of best run were applied voltage 45 V, electrolyte concentration 25 wt.%, stand-off-distance 1.5 mm, pulse frequency 400 Hz and pulse-on-time 45 μs (A_1-B_3-C_3-D_3-E_1). Therefore, the outcome of MRR, OC and TWR were 49.040 mg/h, 108.951 μm and 0.096 mg/h respectively.

However, in order to ensure the result obtained from Table 5, further evaluation of the multi-response characteristics for the optimal combination of the control factors and their levels was determined by averaging the GRGs.

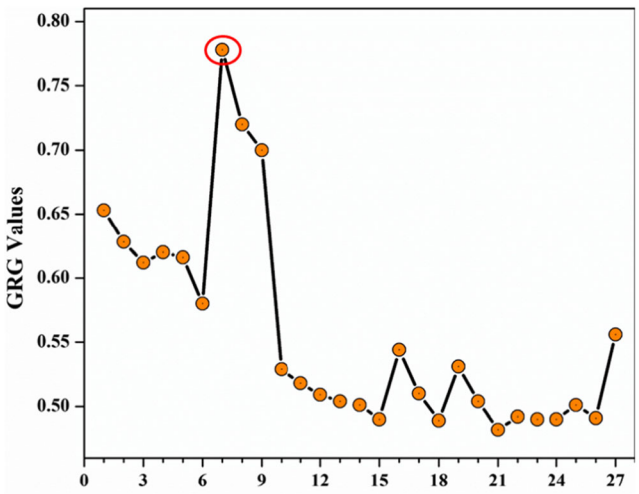

Fig. 8 Main effect plots for GRG (optimum level A_1-B_3-C_3-D_3-E_1)

Table 6 Response table for the GRG

Factor	Process parameter	Level 1	Level 2	Level 3	Total mean of GRG	Optimum level
A	Applied Voltage (V)	**0.656**	0.511	0.504		A_1
B	Electrolyte Conc. (wt.%)	0.552	0.531	**0.588**		B_3
C	Stand-off-distance (mm)	0.545	0.547	**0.579**	0.557	C_3
D	Pulse frequency (Hz)	0.548	0.542	**0.581**		D_3
E	Pulse on time (μs)	**0.572**	0.553	0.545		E_1

Table 6 presents the optimum process parameters for getting good MRR, OC and TWR, hence the optimal combination from GRG is A_1-B_3-C_3-D_3-E_1. Thus, a combination of 45 V applied voltage, 25 wt.% electrolyte concentration, 1.5 mm stand-off-distance, 400 Hz pulse frequency and 45 μs T_{ON} which is same as that observed from Table 5 was achieved.

The graphical representation of the same is depicted through the main effects plot for GRG as shown in Fig. 9. It was noticed that lower applied voltage, higher electrolyte concentration, higher SOD, higher pulse frequency and lower pulse-on-time contributed in increasing the GRG. Generally, the higher the value of GRG, the closer would be ideal value of the product quality [40]. Thus, a higher value of GRG would be desirable for obtaining optimum performance. Therefore, the optimal parametric combination for the maximum MRR and minimum OC and minimum TWR is A_1–B_3–C_3–D_3-E_1 resulted in higher GRG (Fig. 9).

Table 7 represents the ANOVA for MRR, OC and TWR which gives the effective level of selected factors on the desired responses. It was observed that applied voltage is the mostly influencing factor affecting response variables. The electrolyte concentration also marginally influences the MRR, OC and TWR. Furthermore, SOD and pulse frequency have slight effects on the output characteristics. This influence is identified from the percentage contribution calculated at 95% confidence. The interaction effect of all the parameters does not have major effect on the response variables; hence, it is pooled to error.

3.3 Confirmation Test

The confirmation test for the achieved optimum combination was conducted once again to confirm the quality features of producing microchannel in silica glass using ECDM process. Table 5 presents the highest GRG highlighting the combination of control factors as A_1-B_3-C_3-D_3-E_1. Regression equations were formulated as in Eq. 6–8 using MINITAB software to associate the interaction and higher-order effects of the previously mentioned factors, employing the related experimental data as noticed during the course of micro-machining.

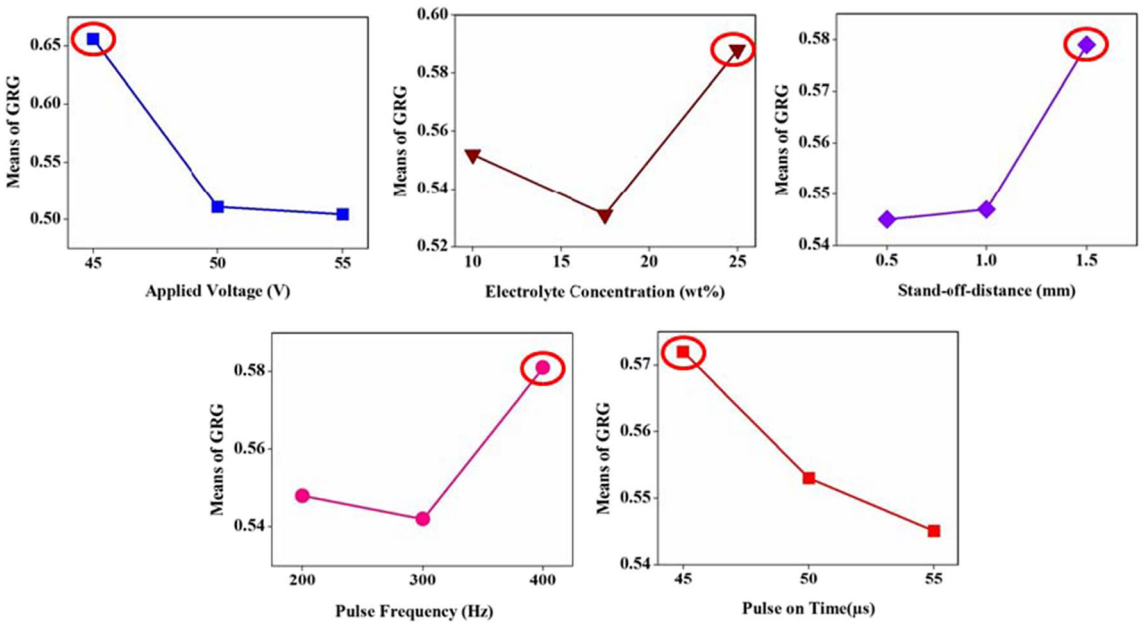

Fig. 9 GRG values vs no. of experiments

Table 7 ANOVA for GRG values

Source	DOF	Seq SS	Adj MS	% contribution	Remarks
Applied Voltage (V)	2	0.1738	0.0869	70.33	Significant
Electrolyte Concentration (wt.%)	2	0.0289	0.0145	11.69	Significant
Stand-off Distance (mm)	2	0.0102	0.0051	4.13	Significant
Pulse frequency (Hz)	2	0.0123	0.0061	4.98	Significant
Pulse on time (μs)	2	0.0049	0.0024	1.98	Insignificant
Residual error	16	0.0170	0.00106	6.89	
Total	26	0.2471			

$$\mathrm{MRR} = -72.8 + 2.547 \times A_1 + 0.506 \times B_3 - 8.31 \times C_3 - 0.0275 \times D_3 + 0.513 \times E_1 \quad (6)$$

$$\mathrm{Overcut} = -175.6 + 5.796 \times A_1 + 1.002 \times B_3 - 16.89 \times C_3 - 0.0632 \times D_3 + 1.311 \times E_1 \quad (7)$$

$$\mathrm{TWR} = -0.1876 + 0.005767 \times A_1 + 0.001050 \times B_3 - 0.01737 \times C_3 - 0.000064 \times D_3 + 0.001316 \times E_1 \quad (8)$$

Table 8 represents comparison between experimental results and predicted results for optimum combination (A_1-B_3-C_3-D_3-E_1). Confirmation experimental results designate a good agreement between the experimental results and predicted values.

3.4 Microstructure Study of Machined Surface

The microstructure investigation of SEM images was carried out on machined surface for optimum combination (A_1-B_3-C_3-D_3-E_1) setting. In every discharge, removal of material from the work piece takes place due to a portion of thermal energy generated in electrolyte concentration. Figure 10a shows the SEM micrograph of microchannel formed in silica glass with a small amount of overcut. Figure 10b, depicts the magnified view in which sharp edges and deep grooves confirmed the material removal in large chunks due to the combination of the applied voltage, concentration and pulse frequency [36]. The relatively smoother surface indicates an improvement in surface roughness. The observed surface roughness was in the range of 1.60 to 3.10 μm. The reproduced micrographs were initial findings, where in the primary focus of study was to determine material removal rate, tool wear rate and overcut. Deep grooves are obtained at several locations due to interlinking of sparks generated during machining. Furthermore, the presence of deeper grooves on the surface due to increase in applied voltage and effect of pulse parameters increases indentation of sparks on machined surface [27, 42]. The presence of fine cracks originating from the shallow grooves confirmed the erosion of material from workpiece. The microstructure examination on machined surface clearly revealed that the dominance of brittle mode of material removal with presence of grain pull-out and fine cracks. Further, the machined surface also appears to be irregular which is attributed to the deposition of re-solidified particles on the previously machined surface which leads to the formation of sharp edges.

4 Conclusion

In the present work ECDM setup has been developed and machining of micro-channel in silica glass using 250 μm tungsten carbide was successfully carried out followed by the optimization of process parameters using GRA. Based on the experimentation results, following conclusions have been drawn.

(i) MRR, OC and TWR to a great extent depend on voltage and electrolyte concentration due to formation of heavily crowded hydrogen bubbles and further coalescence of hydrogen bubbles promotes the occurrence of sparks around the tool vicinity.
(ii) As the stand-off-distance increases MRR, OC and TWR decrease due to the diminished kinetics of electrochemical reactions, resulting in decrease of sparking phenomenon.

Table 8 Predicted and confirmation test results for optimal combination

Output characteristics	Optimal combination	Predicted	Experimental	Error %
MRR (mg/h)	A_1-B_3-C_3-D_3-E_1	54.085	52.109	3.65
Overcut (μm)	(45 V-25 wt.%-1.5 mm-400 Hz-45 μs)	118.65	112.80	4.93
TWR (mg/h)		0.10573	0.0996	5.797

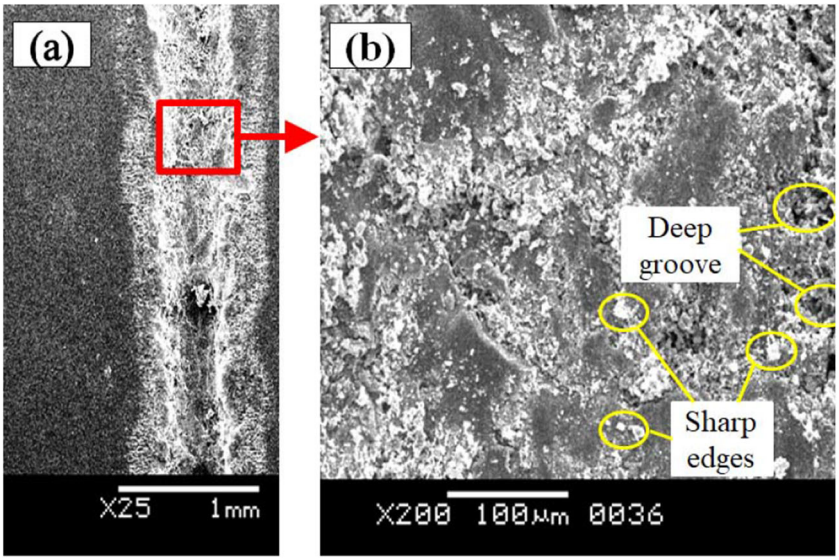

Fig. 10 SEM image of the confirmation test **a** machined groove **b** magnified view

(iii) The optimum combination of control factors obtained through GRA was observed to be A_1-B_3-C_3-D_3-E_1 (45V - 25 wt.% - 1.5 mm – 400 Hz - 45 µs). Further, confirmation experiment results and predicted values were found to be in good agreement with an error 3.65%, 4.93% and 5.797% for MRR, OC and TWR respectively.

(iv) Based on ANOVA results of GRG it was noticed that, applied voltage has major influence on MRR, OC and TWR followed by electrolyte concentration, pulse frequency and SOD.

(v) The microstructural investigation of the machined surface reveals the formation of deep grooves and sharp edges at several locations.

Acknowledgments The authors are thankful to Alva's Institute of Engineering and Technology, Moodabidri, Karnataka, India for permitting to conduct the experimentation work.

Author Contribution All the authors have equally contributed in terms of experimentation, analysis and writing of manuscript.

Funding This work is self-financed and is not funded by any of the government/private/organizations.

Data Availability The datasets generated during and/or analyzed during the current study are available with authors and would be provided to the journal if required.

Declarations

This article does not contain any studies with human participants or animals performed by any of the authors.

Consent to Participate The authors are free to contact any of the people involved in the research to seek further clarification and information. We understand that under freedom of information legalisation and entitled to access the information provided at any time while it is in storage as specified in the manuscript.

Consent for Publication The authors give their consent for the publication of identifiable details, which can include photograph(s) and/or details within the manuscript to be published in Silicon Journal.

Conflict of Interest The authors do not have any conflicts of interest that may have a direct bearing on the subject matter of the article and it will not reflect any possible bias in either the exposition or the conclusions presented.

References

1. Mallick B, Sarkar BR, Doloi B, Bhattacharyya B (2014) Multi criteria optimization of electrochemical discharge micro-machining process during micro-channel generation on glass. Appl Mech Mater 592–594:525–529. https://doi.org/10.4028/www.scientific.net/AMM.592-594.525
2. Singh M, Singh S (2018) Electrochemical discharge machining : a review on preceding and perspective. https://doi.org/10.1177/0954405418798865
3. Alazzam A, Gauthier J, Roman D (2015) Microfluidic device fabrication with serigraphy technique. https://doi.org/10.1177/0954405415615801
4. Castelino P, Shah A, Gokhale M, Jayarama A, Suresh KV, Fernandes P, Pinto R (2021) Optimum hydrogen flowrates and membrane-electrode clamping pressure in hydrogen fuel cells with dual-serpentine flow channels. Materials Today: Proceedings 35: 412–416. https://doi.org/10.1016/j.matpr.2020.02.791
5. Wuthrich R, Fascio V (2005) Machining of non-conducting materials using electrochemical discharge phenomenon - an overview. Int J Mach Tools Manuf 45(9):1095–1108. https://doi.org/10.1016/j.ijmachtools.2004.11.011
6. Sharma P, Mishra DK (2019) Dixit P (2020) Experimental investigations into alumina ceramic micromachining by electrochemical discharge machining process. Procedia Manuf 48:244–250. https://doi.org/10.1016/j.promfg.2020.05.044

7. Furutani K, Maeda H (2008) Machining a glass rod with a lathe-type electro-chemical discharge machine. J Micromech Microeng 18(6). https://doi.org/10.1088/0960-1317/18/6/065006
8. Mediliyegedara TKKR, De Silva AKM, Harrison DK, McGeough JA, Hepburn D (2006) Designing steps and simulation results of a pulse classification system for the electro chemical discharge machining (ECDM) process - an artificial neural network approach. Adv Soft Comput 34:343–352. https://doi.org/10.1007/3-540-31662-0_27
9. Dhanvijay MR, Kulkarni VA, Doke A (2019) Experimental investigation and analysis of electrochemical discharge machining (ECDM) on fiberglass reinforced plastic (FRP). J Inst Eng Ser C. https://doi.org/10.1007/s40032-019-00524-y
10. Bellubbi S, Hipparagi MA, Naik R, Sathisha N (2021, February) Optimization of process parameters in electro chemical discharge machining of silica glass through analysis of means. In IOP Conference Series: Materials Science and Engineering (Vol. 1065, No. 1, p. 012003). IOP Publishing. https://iopscience.iop.org/article/10.1088/1757-899X/1065/1/012003/pdf
11. Mallick B, Hameed AS, Sarkar BR, Doloi B, Bhattacharyya B (2020) Experimental investigation for improvement of micro-machining performances of μ-ECDM process. Materials Today: Proceedings 27:620–626. https://doi.org/10.1016/j.matpr.2019.12.195
12. Torabi A, Razfar MR (2021) The capability of ECDM in creating effective microchannel on the PDMS. Precis Eng 68(November 2020):10–19. https://doi.org/10.1016/j.precisioneng.2020.11.004
13. Furutani K, Maeda H (2008) Machining a glass rod with a lathe-type electro-chemical discharge machine. J Micromech Microeng 18(6). https://doi.org/10.1088/0960-1317/18/6/065006
14. Sathisha N, Hiremath SS, Shivakumar J (2014) Prediction of material removal rate using regression analysis and artificial neural network of ECDM process. Int J Recent Adv. Mech Eng 3(2):69–81. https://doi.org/10.14810/ijmech.2014.3207
15. Mallick B, Sarkar BR, Doloi B, Bhattacharyya B (2017) Analysis on electrochemical discharge machining during micro-channel cutting on glass. Int. J. Precision Technology 7(1):32–50. https://doi.org/10.1504/IJPTECH.2017.084554
16. Hajian M, Razfar MR, Movahed S (2016) An experimental study on the effect of magnetic field orientations and electrolyte concentrations on ECDM milling performance of glass. Precis Eng 45:322–331. https://doi.org/10.1016/j.precisioneng.2016.03.009
17. Yang C-K, Cheng C-P, Mai C-C, Cheng Wang A, Hung J-C, Yan B-H (2010) Effect of surface roughness of tool electrode materials in ECDM performance. Int J Mach Tools Manuf 50(12):1088–1096. https://doi.org/10.1016/j.ijmachtools.2010.08.006
18. Pawar P, Ballav R, Kumar A (2017) Review on material removal technology of soda-lime glass material. Indian J Sci Technol 10(8):1–7. https://doi.org/10.17485/ijst/2017/v10i8/102698
19. Garg MP, Singh M, Singh S (2019, May) Micromachining and process optimization of electrochemical discharge machining (ECDM) process by GRA method. International Scientific-Technical Conference Manufacturing. Springer, Cham, pp 384–392. https://doi.org/10.1007/978-3-030-16943-5_33
20. Badiger RI, Narendranath S, Srinath MS (2019) Optimization of process parameters by Taguchi Grey relational analysis in joining Inconel-625 through microwave hybrid heating. Metallog Microstruct Anal 8(1):92–108. https://doi.org/10.1007/s13632-018-0508-4
21. Naik G, Narendranath S (2018) Optimization of wire-ED turning process parameters by Taguchi-grey relational analysis, i-manager's. J Mech Eng 8(1). https://doi.org/10.26634/jme.8.2.14206
22. Bellubbi S, Sathisha N (2018, June) Reduction in through put time of drum shell manufacturing by single-V welding configuration. In IOP Conference Series: Materials Science and Engineering (Vol. 376, No. 1, p. 012104). IOP Publishing. https://iopscience.iop.org/article/10.1088/1757-899X/376/1/012104/pdf
23. Sathisha N, Somashekhar SH, Shivakumar J, Badiger RI (2013) Parametric optimization of electro chemical spark machining using Taguchi based Grey relational analysis. IOSR Journal of Mechanical and Civil Engineering (IOSR-JMCE):46–52
24. Rajput V, Pundir SS, Goud M, Suri NM (2020) Multi-response optimization of ECDM parameters for silica (quartz) using grey relational analysis. Silicon:1–22. https://doi.org/10.1007/s12633-020-00538-7
25. Paul L, Kumar AB (2018) Improvement in micro feature generation in ECDM process with powder mixed electrolyte. ASME 2018, 13th Int. Manuf. Sci. Eng. Conf. MSEC 2018, vol 4, pp 1–6. https://doi.org/10.1115/MSEC2018-6348
26. Paul L, Antony D (2018) Effect of tool diameter in ECDM process with powder mixed electrolyte. IOP Conference Series: materials science and engineering (vol 396, no 1, p 012070). IOP Publishing
27. Paul L, Hiremath SS (2014) Evaluation of process parameters of ECDM using grey relational analysis. Procedia Mater Sci 5:2273–2282
28. Nagaraj Y, Jagannatha N, Sathisha N, Niranjana SJ (2020) Prediction of material removal rate and surface roughness in hot air assisted hybrid machining on sodalime-silica glass using regression analysis and artificial neural network. Silicon:1–13. https://doi.org/10.1007/s12633-020-00729-2
29. Singh B, Vaishya RO Analyses of output parameters of ECDM using different abrasives-A review. Int J Mater Sci 12(2):307–314, 2017, [Online]. Available: http://www.ripublication.com
30. Elhami S, Razfar MR (2018) Effect of ultrasonic vibration on the single discharge of electrochemical discharge machining. Mater Manuf Process 33(4):444–451. https://doi.org/10.1080/10426914.2017.1328113
31. Bellubbi S, Vijeath A, Mithesh Gowda JR, Prabhu K (2019) Experimental investigation of process parameters on machining force, MRR and power in turning of AISI 316 steel. Int J Comput Aided Manuf 5(1):18–25p
32. Naik GM, Anjan BN, Badiger RI, Bellubbi S, Mishra DK (2021) An investigation on effects of wire-EDT machining parameters on surface roughness of INCONEL 718. Materials Today: Proceedings 35:474–477. https://doi.org/10.1016/j.matpr.2020.03.031
33. Sreenivasulu R, Rao CS (2013) Design of experiments based Grey relational analysis in various machining processes - a review. Res J Eng Sci 2(1):21–26
34. Viswanathan R, Ramesh S, Maniraj S, Subburam V (2020) Measurement and multiresponse optimization of Turning parameters for magnesium alloy using hybrid combination of Taguchi-GRA- PCA technique. Measurement 159:107800. https://doi.org/10.1016/j.measurement.2020.107800
35. Sachin B, Narendranath S, Chakradhar D (2018) Experimental evaluation of diamond burnishing for sustainable manufacturing. Mater Res Exp 5(10):106514
36. Sindhu D, Thakur L, Chandna P (2019) Multi-objective optimization of rotary ultrasonic machining parameters for quartz glass using Taguchi-Grey relational analysis (GRA). Silicon 11(4):2033–2044. https://doi.org/10.1007/s12633-018-0019-6
37. Jahan MP, Rahman M, Wong YS (2014) Micro-electrical discharge machining (Micro-EDM): Processes, varieties, and applications, vol 11. Elsevier
38. Jawalkar CS, Sharma AK, Kumar P (2020) Innovations in electro chemical discharge machining process through electrolyte stirring and tool rotations. Int J Mach Mach Mater 22(6):487–503. https://doi.org/10.1504/IJMMM.2020.111354
39. Jui SK, Kamaraj AB, Sundaram MM (2013) High aspect ratio micromachining of glass by electrochemical discharge machining

(ECDM). J Manuf Process 15(4):460–466. https://doi.org/10.1016/j.jmapro.2013.05.006

40. Nagaraj Y, Jagannatha N, Sathisha N, Niranjana SJ (2021) Parametric optimization on hot air assisted hybrid machining of soda-lime glass using Taguchi based grey relational analysis. Multiscale Multidiscip Model Exp Des. https://doi.org/10.1007/s41939-020-00085-z
41. Stalin B, Kumar PR, Ravichandran M, Kumar MS, Meignanamoorthy M (2019) Optimization of wear parameters using Taguchi grey relational analysis and ANN-TLBO algorithm for silicon nitride filled AA6063 matrix composites. Mater Res Exp 6(10):106590. https://doi.org/10.1088/2053-1591/ab3d90
42. Bindu Madhavi J, Hiremath SS (2019) Machining and characterization of channels and textures on quartz glass using μ-ECDM process. Silicon 11(6):2919–2931. https://doi.org/10.1007/s12633-019-0083-6